European Journal of Radiology Open 14 (2025) 100622

Contents lists available at ScienceDirect

European Journal of Radiology Open

journal homepage: www.elsevier.com/locate/ejro

Deep learning enabled near-isotropic CAIPIRINHA VIBE in the nephrogenic phase improves image quality and renal lesion conspicuity

Qinxuan Tan [a], Jingyu Miao [a], Leila Nitschke [a], Marcel Dominik Nickel [c], Markus Herbert Lerchbaumer [a], Tobias Penzkofer [a,b], Sebastian Hofbauer [d], Robert Peters [d], Bernd Hamm [a], Dominik Geisel [a], Moritz Wagner [a], Thula Cannon Walter-Rittel [a,*]

[a] Department of Radiology, Charité - Universitätsmedizin Berlin, Freie Universität Berlin, Humboldt-Universität zu Berlin, and Berlin Institute of Health, Berlin, Germany
[b] Berlin Institute of Health, Berlin, Germany
[c] MR Application Predevelopment, Siemens Healthnineers, Forchheim, Germany
[d] Department of Urology, Charité - Universitätsmedizin Berlin, Freie Universität Berlin, Humboldt-Universität zu Berlin, and Berlin Institute of Health, Berlin, Germany

HIGHLIGHTS

- DL-CAIPIRINHA-VIBE improves image quality compared to standard CAIPIRINHA-VIBE.
- DL-CAIPIRINHA-VIBE lends itself to high-resolution and high-quality MPR.
- DL-CAIPIRINHA-VIBE is less susceptible to breath-hold artifacts, which improves image quality.

ARTICLE INFO

Keywords:
Deep learning
Magnetic resonance imaging
Renal lesions
Multi-planar reconstructions
Image quality

ABSTRACT

Background: Deep learning (DL) accelerated controlled aliasing in parallel imaging results in higher acceleration (CAIPIRINHA)-volumetric interpolated breath-hold examination (VIBE), provides high spatial resolution T1-weighted imaging of the upper abdomen. We aimed to investigate whether DL-CAIPIRINHA-VIBE can improve image quality, vessel conspicuity, and lesion detectability compared to a standard CAIPIRINHA-VIBE in renal imaging at 3 Tesla.

Methods: In this prospective study, 50 patients with 23 solid and 45 cystic renal lesions underwent MRI with clinical MR sequences, including standard CAIPIRINHA-VIBE and DL-CAIPIRINHA-VIBE sequences in the nephrographic phase at 3 Tesla. Two experienced radiologists independently evaluated both sequences and multiplanar reconstructions (MPR) of the sagittal and coronal planes for image quality with a Likert scale ranging from 1 to 5 (5 =best). Quantitative measurements including the size of the largest lesion and renal lesion contrast ratios were evaluated.

Results: DL-CAIPIRINHA-VIBE compared to standard CAIPIRINHA-VIBE showed significantly improved overall image quality, higher scores for renal border delineation, renal sinuses, vessels, adrenal glands, reduced motion artifacts and reduced perceived noise in nephrographic phase images (all $p < 0.001$). DL-CAIPIRINHA-VIBE with MPR showed superior lesion conspicuity and diagnostic confidence compared to standard CAIPIRINHA-VIBE. However, DL-CAIPIRINHA-VIBE presented a more synthetic appearance and more aliasing artifacts ($p < 0.023$). The mean size and signal intensity of renal lesions for DL-CAIPIRINHA-VIBE showed no significant differences compared to standard CAIPIRINHA-VIBE ($p > 0.9$).

Abbreviations: MRI, Magnetic resonance imaging; CT, computed tomography; DL, deep learning; CAIPIRINHA, controlled aliasing in parallel imaging results in higher acceleration; VIBE, volume interpolated breath-hold examination; SNR, signal to noise ratio; SI, signal intensity; RRC, renal lesion contrast; ROI, region of interest; RCC, renal cell carcinoma; MPR, multi-planar reconstruction; I.v., intravenous.

* Correspondence to: Department of Radiology, Charité - Universitätsmedizin Berlin Charité Platz 1, Berlin 10117, Germany.
E-mail addresses: qinxuan.tan@charite.de (Q. Tan), jingyu.miao@charite.de (J. Miao), marcel.nickel@siemens-healthineers.com (M.D. Nickel), markus.lerchbaumer@charite.de (M.H. Lerchbaumer), tobias.penzkofer@charite.de (T. Penzkofer), Sebastian.hofbauer@charite.de (S. Hofbauer), Robert.peters@charite.de (R. Peters), bernd.hamm@charite.de (B. Hamm), moritz.wagner@charite.de (M. Wagner), thula.walter-rittel@charite.de (T.C. Walter-Rittel).

https://doi.org/10.1016/j.ejro.2024.100622
Received 12 October 2024; Received in revised form 3 December 2024; Accepted 8 December 2024
Available online 12 December 2024

Conclusions: DL-CAIPIRINHA-VIBE is well suited for kidney imaging in the nephrographic phase, provides good image quality, improved delineation of anatomic structures and renal lesions.

1. Introduction

Magnetic resonance imaging (MRI) is well-established in the evaluation and characterization of renal lesions. Compared to computed tomography (CT), MRI offers higher specificity for small renal lesions (<2 cm), superior contrast resolution, and no ionizing radiation [1–3]. In clinical practice, high spatial resolution imaging with the capability of multiplanar reconstruction (MPR) is essential for optimal assessment of the kidney [4]. To this end, contrast-enhanced T1-weighted sequences are widely accepted as essential for detecting and characterizing renal lesions and are typically performed with breath-hold three-dimensional (3D) gradient echo sequences, such as Volumetric Interpolated Breath-hold Examination (VIBE) [5,6]. Despite the use of advanced parallel imaging acceleration techniques like Controlled Aliasing in Parallel Imaging Results in Higher Acceleration (CAIPIRINHA), challenges remain in achieving high spatial resolution with breath-hold acquisitions without compromising signal-to-noise ratio (SNR) and overall image quality [6–8]. Reduced spatial resolution and SNR can in turn affect the image quality of MPR, which rely on high-quality isotropic data for accurate visualization and depiction of renal structures in multiple planes. Poor spatial resolution and non-isotropic datasets as well as reduced SNR are detrimental to the image quality of MPR [9].

Recently, deep learning (DL) reconstruction algorithms have proven feasible in reducing acquisition time as well as improving both image quality and signal-to-noise ratios (SNR) in MRI [10]. DL reconstruction is a versatile method applicable both in-line and off-line within the image-reconstruction pipeline for various upper abdominal sequences including T2-, T1-, and diffusion-weighted imaging [11–13]. Integration of DL reconstruction with 3D T1-weighted sequences was reported on from various vendors on 1.5 and 3Tesla scanners [14–16]. Recently, DL-CAIPIRINHA-VIBE with an acceleration factor of 6 was introduced to achieve high isotropic spatial resolution breath-hold imaging of the liver and demonstrated very promising results[17]. In this study however, DL-CAIPIRINHA-VIBE was only evaluated for non-enhanced and hepatobiliary images after i.v. application gadoxetic acid for the detection of liver lesions. To the best of our knowledge our study is the first to describe DL-CAIPIRINHA-VIBE and its' MPRs in renal imaging.

The aim of this study was to compare DL-CAIPIRINHA-VIBE standard CAIPIRINHA-VIBE at 3 Tesla with respect to image quality and lesion detection in kidney imaging in the acquired axial plane as well as the reconstructed sagittal and coronal planes.

2. Materials and methods

The local ethics committee approved this prospective study. Written and informed consent was obtained from all patients prior to the examination.

2.1. Patients

In this prospective study, 50 consecutive patients were enrolled from June 2021 to June 2023 (male 28, 56 %; female 22, 44 %). All of whom underwent upper abdominal MRI with the addition of the DL-CAIPIRINHA-VIBE for various clinical indications (referral for renal and non-renal pathologies). Mean patient age was 61.7 ± 15.5 years (range 22–87 years). Inclusion criteria were the ability to provide informed consent, patient age > 18 years. Exclusion criteria were contraindications to MRI or intravenous contrast application, patient age < 18 years, previous bilateral nephrectomy, inability to provide informed consent. Aggregated patient data is provided in Table 1.

2.2. MR system and sequence parameters

All MRI examinations were performed on a clinical 3 Tesla MR scanner (MAGNETOM Vida; Siemens Healthcare, Erlangen, Germany) using an 18-channel body and/or 32-channel spine array. Routine upper abdominal MRI protocols involved T1-weighted dual-echo imaging, pre- and post-contrast imaging, T2-weighted imaging with and without fat-suppressed, and diffusion-weighted imaging using two b-values (50, 400 s/mm^2). Dynamic imaging including the corticomedullary phase, nephrographic phase, and delayed phase, was performed using 3D fat-suppressed (fs) VIBE sequence, following the intravenous administration of 0.1 mmol/kg gadolinium-based extracellular contrast agent (gadobutrol, Gadovist, Bayer Pharma AG, Berlin, Germany or gadoteric acid, Dotarem, Guerbet, Villepinte, France). All exams included the standard DL-CAIPIRINHA-VIBE sequence in the nephrographic phase as an addition to our standard renal protocol, which also included the standard CAIPIRINHA-VIBE in the nephrographic phase. Sequence parameters of CAPIRINHA-VIBE and DL-CAPIRINHA-VIBE are provided in Table 2.

The DL reconstruction algorithm for the CAIPIRINHA-VIBE was employed using a research application which has been previously described by Wei et al. and involves two sequential, independent processing steps [17]. First, images were reconstructed from under-sampled k-space data using a network inspired by variational networks [16], which also incorporated coil sensitivity maps estimated from calibration scans. The network parameters were previously determined through supervised training using approximately 5000 training pairs derived from approximately 500 fully sampled 3D datasets acquired from healthy volunteers on 1.5 and 3 Tesla MRI scanners (MAGNETOM scanners, Siemens Healthineers, Erlangen, Germany) in the head, abdomen, and pelvis. In a second step, the reconstructed images were interpolated using a DL-based super-resolution algorithm that up-samples images by a factor of 2 in all spatial dimensions and that is optimized for the given partial Fourier sampling. First, images were

Table 1
Aggregated Patient data. Renal lesions marked with an * were confirmed by histology. Cystic lesions were classified with the Bosniak classification system.

Patient Characteristics	
Demographics	
Male	28 (56 %)
Female Age (Mean ± Std dev., [Range])	22 (44 %)
	61.7 ± 15.5 [22–87]
Lesions	
Single renal lesion	38 (76 %)
Multiple renal lesions	12 (24 %)
Solid Lesions	23 (33.8 %)
benign	9 (39.1 %)
Angiomyolipoma	7
Oncocytoma*	2*
Malignant	14 (60.9 %)
renal cell carcinoma (4 ccRCC*, 1 pRCC*, 8 FU)	13
malignant epitheloid angiomyolipoma*	1*
Cystic Lesions	45 (66.2 %)
Bosniak I	19
Bosniak II	17
Bosniak IIF	7
Bosniak III (FU)	1
Bosniak IV (Oncocytoma*)	1*

ccRCC (clear cell renal carcinoma), FU (follow-up), pRCC (papillary renal cell carcinoma), Std.dev (Standard deviation)

Table 2
CAIPIRINAHA-VIBE and DL-CAIPIRINAHA-VIBE acquisition parameters.

	CAIPIRINAHA-VIBE	DL-CAIPIRINAHA-VIBE
Orientation	Axial	Axial
Repetition Time	4.0	3.4
Echo Time	1.3	1.3
Flip Angle	9	9
Receiver Bandwidth	1042	444
FOV	380 × 309*	420 x 334*
Matrix	317 x 258	350 x 278
Voxel Size (mm^3)	1.2 × 1.2 × 3.0	1.2 × 1.2 × 1.2
Number of Slices	72	186
Slice Thickness (mm)	3.0	1.2
Acceleration factor	4	6
Acquisition Time	14	16

* FOV in this table is the default value, which was individually adjusted.

reconstructed from under-sampled k-space data using a network inspired by variational networks, which also incorporated coil sensitivity maps estimated from calibration scans. The network architecture was implemented in PyTorch (Linux Foundation, San Fransisco, CA, USA). Supervised training had been performed with approximately 5000 training pairs derived from approximately 500 fully sampled 3D datasets acquired from healthy volunteers on 1.5 and 3 Tesla MRI scanners (MAGNETOM scanners, Siemens Healthcare) in the head, abdomen, and pelvis [18]. In a second step, the reconstructed images were interpolated using a DL-based super-resolution algorithm, by initially up-sampling the images by a factor of 2 in all spatial dimensions and performing partial Fourier reconstruction, trained on high-resolution images down sampled for input data.

2.3. Qualitative image assessment

Image quality was qualitatively evaluated for standard VIBE and DL-VIBE in the axial plane and MPRs in the sagittal and coronal planes. Two experienced radiologists (>10 years of experience) independently evaluated these images. Both readers were blinded to patient history, clinical information, pathology results, and the original MRI report. Image evaluation was performed on a clinical workstation using Visage 7 (Visage Imaging GmbH, Berlin, Germany). Imaging assessment parameters included overall image quality, sharpness of renal borders, renal sinuses, adrenal gland conspicuity, renal vessel conspicuity, respiratory motion artifacts, aliasing artifacts, perceived noise, synthetic image appearance, delineation of renal lesions and diagnostic confidence on Likert 5-poing scale (Table 3).

2.4. Lesion conspicuity and detection evaluation

To objectively evaluate lesion-to-kidney contrast, every reader independently placed a circular region of interest (ROI) in each solid lesion, the largest diameter of a cystic lesion and within the adjacent renal parenchymal, on standard CAIPIRINHA-VIBE and DL-CAIPIRINHA-VIBE images. The ROI was chosen manually to cover the entire lesion. The ROI diameter to assess renal parenchyma was approximately 10 mm (10.07 ± 0.13 mm, 9.81–10.38 mm). The contrast ratio between renal parenchyma and the renal lesion (RRC) was calculated by the following formula as previously published by Fahlenkamp et al. [19]:

$$RRC = (SI_{renal} - SI_{lesion})/SI_{renal}$$

2.5. Statical analysis

Statistical analysis was performed using R (Version 4.4.1, R Foundation, Vienna, Austria). Continuous variables were reported as mean with standard deviation, and ordinal variables were described using the median and interquartile range (IQR). The Kolmogorov-Smirnov test was used to assess normality of variables. The paired Wilcoxon signed-rank test was applied to compare image quality between DL-CAPIRINHA-VIBE and standard CAIPIRINHA-VIBE sequences. Continuous variables were compared using the *t*-test or Wilcoxon test for skewed distributions. Inter-observer agreement was evaluated with intraclass correlation coefficient (ICC) or Cohen's Kappa. Based on the 95 % confidence interval [2] of the ICC estimate, reliability was defined as follows: 0–0.50 = poor reliability, 0.51–0.75 = moderate reliability, 0.76–0.90 = good reliability, 0.91–1.00 = excellent reliability. A two-sided p-value less than 0.05 was considered statistically significant [20].

3. Results

3.1. Patients and lesions

For the 50 included patients, MRI examinations showed 68 detectable focal solid and/or cystic renal lesions (solid lesions: 23, 33.8 %; cystic lesions: 45, 66.2 %). Aggregated patient data and lesion data is provided in Table 1. Renal lesions were diagnosed based both characteristic MR imaging findings for Bosniak I-IIF cysts and angiomyolipomas. Two solid lesions were confirmed to be oncocytomas upon resection (n = 2). 8 of the 14 solid malignant lesions were diagnosed based on imaging findings, a history of previous RCC and follow-up in an

Table 3
Scoring criteria for image assessment.

Parameter	Score 1	2	3	4	5
Image Quality	Non-diagnostic	Poor	Moderate	Good	Excellent
Sharpness of Organs	Not delineated	severe blurring	Moderate blurring	Good delineation	Sharpest border
Renal Vessel Conspicuity	Not delineated	Entire vessels system was shown with severe blurring	Entire vessels system was shown with moderate blurring	1st-order branches were well delineated with clear margin	1st- and 2nd-order branches were well delineated with clear margin
Artifact	Non-diagnostic	severe artifacts compromising diagnostic evaluation	Small to moderate artifact	Visible but minor artifact	No artifact
Perceived Noise	Non-diagnostic	Marked noise level	Moderate noise level	Mild noise level	Negligible noise level
Synthetic Appearance	Non-diagnostic	Severe	Moderate	Mild	No synthetic appearance
Delineation of Renal Lesions	Not delineated	severe blurring	Moderate blurring	Good delineation	Sharpest border
Diagnostic Confidence	Non-diagnostic	Poor	Moderate	Good	Excellent

oncological setting. The Bosniak III cyst was followed up upon due to patient preferences. The single Bosniak IV cyst was proven to be an oncocytoma upon resection.

3.2. Qualitative evaluation of image quality

Comprehensive results from both readers are provided in Tables 4 and 5. Both readers consistently assigned higher scores for overall image quality to the DL-CAIPIRINHA-VIBE compared to standard CAIPIRINHA-VIBE ($p < 0.001$). DL-CAIPIRINHA-VIBE and MPR sequences provided good to excellent delineation of renal borders, renal sinuses, renal vessels and the adrenal glands. All these scores were significantly higher compared to the standard VIBE sequence ($p < 0.001$, Figs. 1–3**)**. For both readers, the DL-CAIPIRINHA-VIBE MPRs showed significantly less perceived noise than the standard CAIPIRINHA-VIBE MPR ($p < 0.001$).

DL-CAIPIRINHA-VIBE (median, 5; IQR: 5, 5) showed significantly better scores for respiratory motion artifacts compared to conventional VIBE (median, 4; IQR: 4, 5) ($p < 0.001$). In contrast, aliasing artifacts were observed more frequently in DL-CAIPIRINHA-VIBE (median, 5; IQR: 4,5) compared to conventional CAIPIRINHA-VIBE (median, 5; IQR: 5,5) ($p = 0.003$). The observed artifacts were typically mild and did not affect diagnostic image quality (Fig. 4). Synthetic appearance was more pronounced for DL-CAIPIRINHA-VIBE compared to standard CAIPIRINHA-VIBE, but the overall effect was mild (median: 5; IQR: 4, 5; $p < 0.023$).

3.3. Lesion assessment

The comparison of lesion delineation and diagnostic confidence for DL-CAIPIRINHA-VIBE and standard VIBE images are detailed in Table 4 and Table 5. DL- CAIPIRINHA-VIBE demonstrated significantly higher scores for delineation and diagnostic confidence compared with the standard CAIPIRINHA-VIBE sequences ($p < 0.001$).

There was no significant difference in lesion sizes between DL-CAIPIRINHA-VIBE and standard CAIPIRINHA-VIBE, the Bland-Altmann plot from two readers as shown in Fig. 5. Reader 1: mean renal lesion size in standard CAIPIRINHA-VIBE was 28.1 ± 26.9 (SD) mm (range: 4.5 −132.0 mm) vs. 28.0 ± 26.8 (SD) mm (range: 4.8 −131.3 mm) in DL- CAIPIRINHA-VIBE ($p = 0.922$). Reader 2, mean renal lesion size in standard CAIPIRINHA-VIBE 28.0 ± 26.8 (SD) mm (range: 5.1 −130.2 mm) vs. 28.5 ± 26.8 (SD) mm (range: 5.0 −129.1 mm) in DL- CAIPIRINHA-VIBE ($p = 0.906$).

Table 5
P value of image quality scores for comparing CAIPIRINHA-VIBE and DL-CAIPIRINHA-VIBE.

	CAIPIRINHA-VIBE ax Vs. DL-CAIPIRINHA-VIBE ax		CAIPIRINHA-VIBE MPR Vs. DL-CAIPIRINHA-VIBE MPR	
	Reader 1	Reader 2	Reader 1	Reader 2
Overall Image Quality	< 0.001	< 0.001	< 0.001	< 0.001
Delineation of Renal edge	< 0.001	< 0.001	< 0.001	< 0.001
Delineation of Renal Sinus	< 0.001	< 0.001	< 0.001	< 0.001
Delineation of Renal vessels	< 0.001	< 0.001	< 0.001	< 0.001
Adrenal Gland	< 0.001	< 0.001	< 0.001	< 0.001
Perceived Noise	0.331	< 0.001	< 0.001	< 0.001
Synthetic Appearance	< 0.001	< 0.001	< 0.001	0.023
Delineation of Renal Lesion	< 0.001	< 0.001	< 0.001	< 0.001
Diagnostic Confidence	< 0.001	< 0.001	< 0.001	< 0.001

ax (axial), DL (deep learning), MPR (multiplanar reconstruction)

Mean renal lesion contrast ratio (RRC) was com for both sequences (0.61 ± 0.29 on standard CAIPIRINHA-VIBE vs. 0.63 ± 0.25 on DL-CAIPIRINHA-VIBE; $p = 0.240$). For solid renal lesions, RCC was superior for DL-CAIPIRINHA-VIBE compared to standard CAIPIRINHA-VIBE (0.35 ± 0.16 vs. 0.27 ± 0.20; ($p = 0.005$)). For cystic lesions, RRC was comparable between the two sequences (0.81 ± 0.10 and 0.81 ± 0.09; standard CAIPIRINHA-VIBE vs. DL-CAIPIRINHA-VIBE respectively ($p = 0.617$)).

3.4. Interobserver agreement

All ICC results from the two readers are shown in Table 4. Interobserver agreement for image quality ranged from moderate to good in DL-CAIPIRINHA-VIBE (ICC range, 0.508–0.875). In terms of perceived noise, the ICC score was poor for both standard CAIPIRINHA-VIBE and DL-CAIPIRINHA-VIBE (ICC range 0.224–0.495).

4. Discussion

We were able to show that contrast enhanced DL-CAIPIRINHA-VIBE in the nephrographic phase provides excellent image quality, superior detectability and diagnostic confidence in the assessment of both solid and cystic renal lesions compared to a standard CAIPIRINHA-VIBE sequence. With an acceleration factor of 6, DL-CAIPIRINHA-VIBE also achieves greater isotropic spatial resolution (1.2 ×1.2 ×1.2 mm^3) at a comparable breath hold time of 16 s compared to the 14 s for the

Table 4
Comparisons of image quality scores between CAIPIRINHA-VIBE and DL-CAIPIRINHA-VIBE on nephrographic images.

	CAIPIRINHA-VIBE ax		DL-CAIPIRINHA-VIBE ax		CAIPIRINHA-VIBE MPR		DL-CAIPIRINHA-VIBE MPR	
	Reader 1	Reader 2	Reader 1	Reader 2	Reader 1	Reader 2	Reader 1	Reader 2
Overall Image Quality	4 [4–4.75]	4 [4,5]	5 [4,5]	5 [5]	3 [3,4]	3 [3,4]	4 [4,5]	5 [4,5]
ICC	0.445		0.796		0.535		0.579	
Delineation of Renal edge	4 [4,5]	4 [4,5]	5 [5]	5 [5]	4 [3.25–4]	4 [4]	5 [4,5]	5 [5]
ICC	0.623		0.585		0.505		0.612	
Delineation of Renal Sinus	4 [4]	4 [4]	5 [5]	5 [5]	3 [3,4]	4 [3,4]	5 [4,5]	5 [4,5]
ICC	0.532		0.690		0.693		0.743	
Renal vessel Conspicuity	4 [4]	4 [4]	5 [5]	5 [5]	3 [3,4]	4 [3,4]	5 [4,5]	5 [4,5]
ICC	0.692		0.641		0.553		0.710	
Adrenal Gland	4 [3,4]	4 [3,4]	5 [4,5]	5 [4,5]	3 [2,3]	3 [3,4]	4 [4–4.75]	4 [4,5]
ICC	0.719		0.875		0.291		0.548	
Perceived Noise	5 [4,5]	5 [4,5]	5 [4,5]	5 [5]	3 [3]	3 [3,4]	5 [4,5]	5 [4,5]
ICC	0.495		0.224		0.807		0.598	
Synthetic Appearance	5 [5]	5 [5]	5 [4,5]	4.5 [4,5]	5 [4,5]	5 [4,5]	4 [4,5]	4 [4,5]
ICC	0.509		0.833		0.645		0.750	
Delineation of Renal Lesion	4 [4,5]	4 [4,5]	5 [5]	5 [5]	4 [3,4]	4 [3,4]	5 [4,5]	5 [5]
ICC	0.471		0.508		0.591		0.562	
Diagnostic Confidence	4.5 [4,5]	4 [4,5]	5 [5]	5 [5]	3 [3,4]	4 [3,4]	5 [4,5]	5 [5]
ICC	0.536		0.660		0.584		0.665	

ax (axial), ICC (intraclass correlation coefficient), MPR (multiplanar reconstruction)

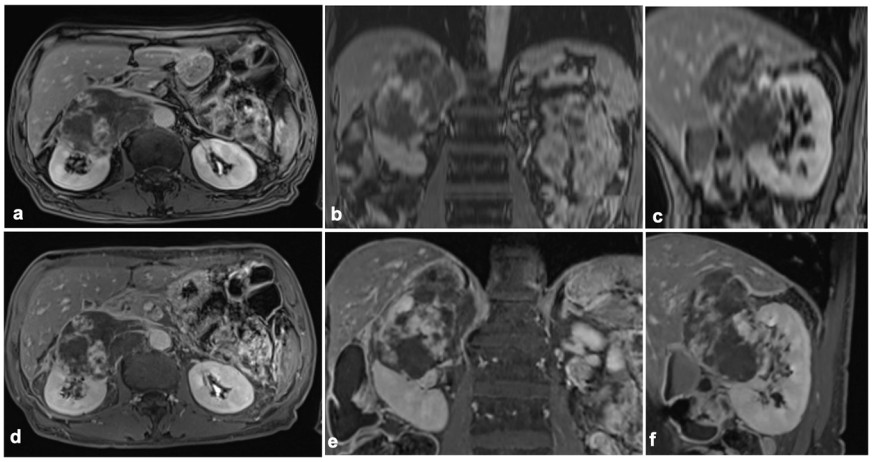

Fig. 1. Nephrographic phase MRI of a 68-year-old male patient with malignant epithelioid angiomyolipoma. The standard CAIPIRINAHA-VIBE axial (a), with MPR coronal (b) sagittal plane (c) in the top row show worse image quality, lesion delineation and vessel conspicuity compared to DL-CAIPIRINAHA-VIBE with MPR imaging (the bottom row; d: axial, e: MPR coronal, f: MPR sagittal).

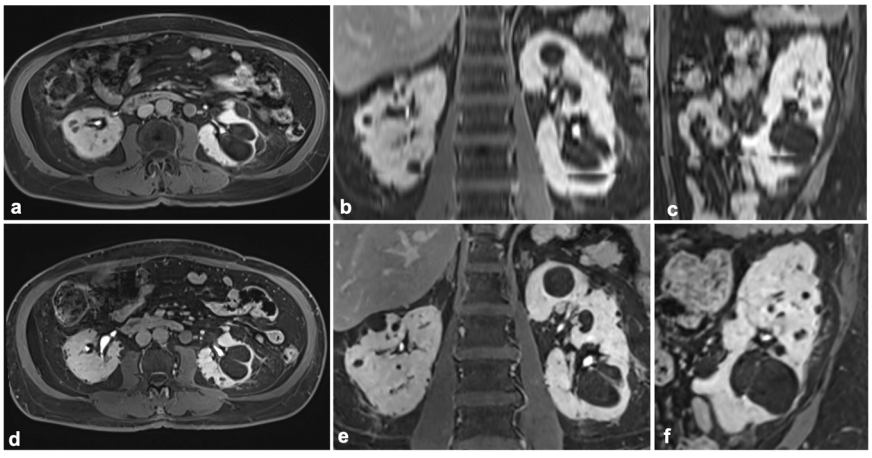

Fig. 2. Nephrographic enhanced phase MRI of a 65-year-old female patient with cystic renal lesions (Bosniak I-IIF). The standard CAIPIRINAHA-VIBE axial (a), with MPR coronal (b) sagittal plane (c) in the top row show worse image quality, lesion delineation and septal conspicuity compared to DL-CAIPIRINAHA-VIBE with MPR imaging (the bottom row; d: axial, e: MPR coronal, f: MPR sagittal).

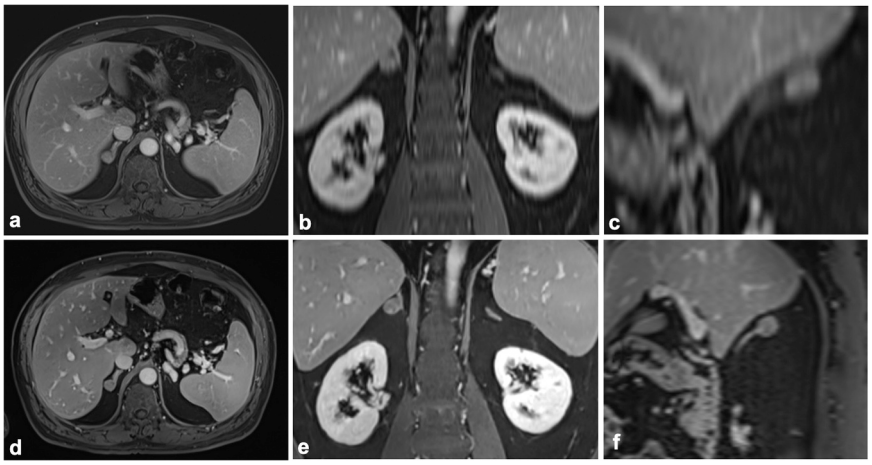

Fig. 3. Both standard CAIPIRINAHA-VIBE (a) and DL-CAIPIRINAHA-VIBE (d) showed excellent (Likert score: 5) image quality and conspicuity of the adrenal gland (with an adenoma) on nephrographic phase imaging. In addition, standard CAIPIRINAHA-VIBE MPR (coronal: b; sagittal: c) showed worse adrenal gland conspicuity compared to and DL-CAIPIRINAHA-VIBE MPR (e: MPR coronal, f: MPR sagittal).

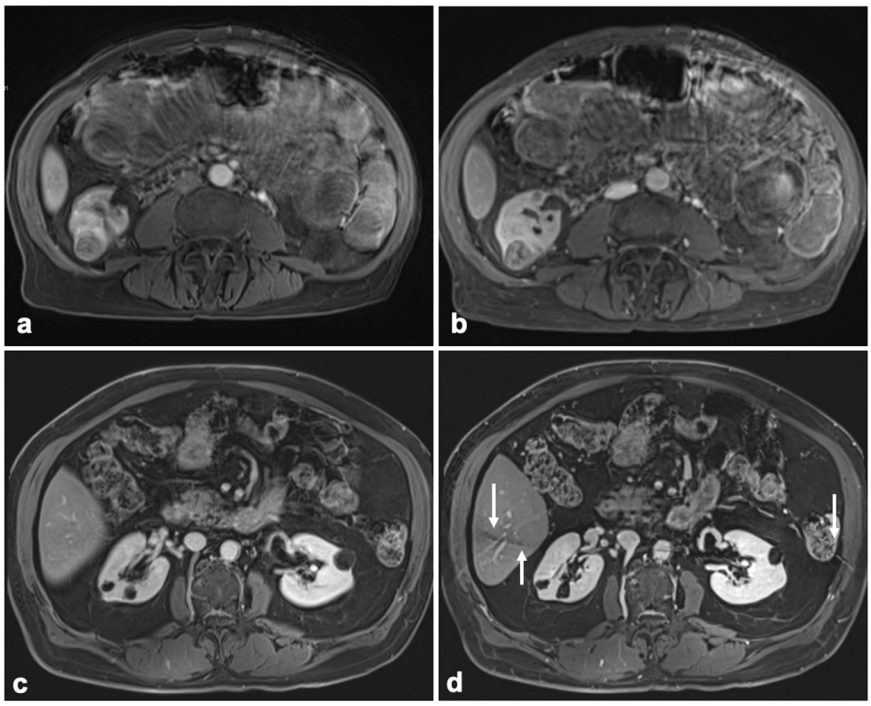

Fig. 4. CAIPIRINAHA-VIBE demonstrated showed more pronounced respiratory motion artifacts (a) compared to DL-CAIPIRINAHA-VIBE (b). In the other hand, aliasing artifacts were observed more frequently in the DL-CAIPIRINHA-VIBE (d vs. c). These artifacts were typically mild and did not affect kidney assessment (arrow).

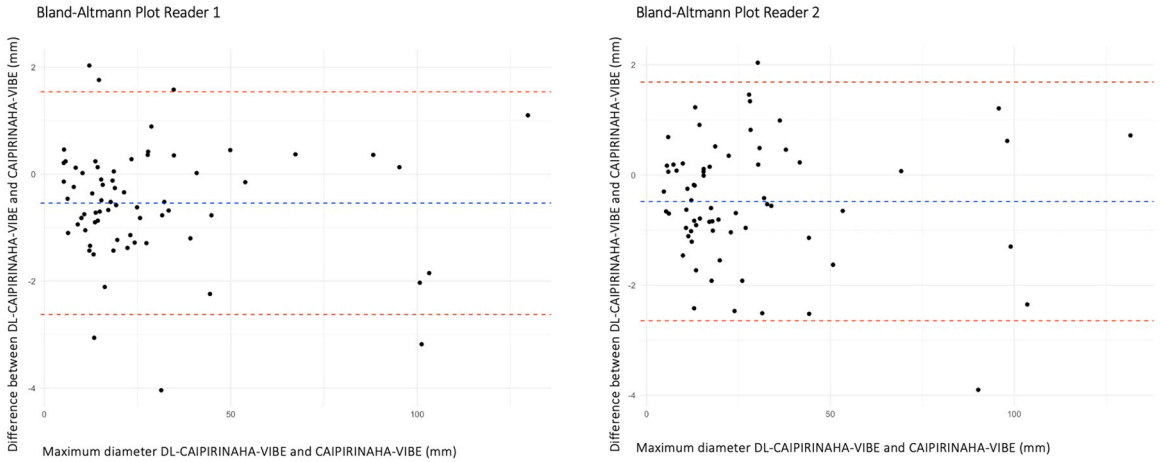

Fig. 5. Bland-Altman plot of maximum measured diameters in DL-CAIPIRINAHA-VIBE compared with CAIPIRINAHA-VIBE by two readers.

standard CAIPIRINHA-VIBE sequence and is therefore well-suited for multiplanar reformation in nephrographic phase images. DL-CAIPIRINHA-VIBE also offered superior image quality with reduced breathing artifacts. Moreover, conspicuity of renal vessels and adrenal glands, which are important anatomic landmarks in renal imaging and staging of kidney tumors, was also improved in DL-CAIPIRINHA-VIBE compared to standard CAIPIRINHA-VIBE.

High spatial resolution imaging and MPR capability are crucial for the optimal assessment of focal renal lesions and can be accomplished by using either CT or MRI [21,22]. MPR improves the visualization of anatomic structures, enabling more accurate diagnosis and assessment of renal pathologies, such as renal anatomy relative to and surrounding organs, lesion location and depth of extension into the kidney, relationship of the tumor to the collection system and precise delineation of the artery and venous anatomy [2].

In abdominal imaging MPRs are typically reconstructed from axial or sagittal isotropica datasets, i.e. (3D) sequences. To achieve high spatial resolution, parallel acquisition techniques such as SENSitivity encoding (SENSE), generalized autocalibration partially parallel acquisition (GRAPPA), and iterative self-consistent parallel imaging (SPIRiT) are widely incorporated into 3D T1-weighted GRE sequences [23–25]. These techniques accelerate image acquisition by exploiting properties of phased-array receiver coil arrays to separate aliased pixels in the image domain or to estimate missing k-space data using knowledge of nearby acquired k-space points. However, in these 3D T1-weighted sequences, high acceleration factors (i.e. >4) cause a loss of signal-to-noise ratio (SNR) and are susceptible to aliasing artifacts [23,25,26]. Compared to these techniques, CAIPIRINHA allows for higher acceleration factors by accelerating data acquisition in both phase encoding and slice encoding direction, leading to shorter acquisition times and reduced image degradation [27]. Previous studies have shown that CAIPIRINHA-VIBE provides superior image quality compared to

conventional GRAPPA technique [14,26–28]. In our study, the standard CAIPIRINHA-VIBE axial plane with an acceleration factor of 4 provided robust image quality; however, its relatively thick slice thickness and low spatial resolution through the plane ($1.2 \times 1.2 \times 3.0\ mm^3$) did not allow reconstruction of optimal MPR images.

The DL-CAIPIRINHA-VIBE utilizes several optimizations, as detailed by Wei et al., including the use of a primary k-space to image construction anchored in a variational network architecture which ensured amplified noise mitigation and artifact suppression [17,23]. In addition to these optimizations, a super-resolution algorithm focused on refining through-plane resolution, specifically tailored for the partial Fourier acquisition as previously described in other studies was employed [29,30]. These improvements led to improved overall image quality, lesion detectability, vessel visibility, and reduction of breath-hold artifacts in DL-CAIPIRINHA-VIBE images, albeit with a more synthetic appearance [17]. Similarly, Song et al. also found improved image quality and SNR in a DL reconstructed near isotropic T1w contrast enhanced sequence in MR enterography, at the expense of a more synthetic image appearance [16]. All these findings are in line with our study, but the effect of synthetic appearance appears was mild in our study (median: 5; IQR: 4, 5; $p < 0.023$).

Overall, our study findings confirmed findings from previous studies on DL-VIBE. These previous studies however, evaluated the DL-CAIPIRINHA-VIBE in the hepatobiliary phase after administration of gadoxetic acid, while we assessed the diagnostic performance of DL-CAIPIRINHA-VIBE in detection of subtle contrast differences typically observed in the renal parenchyma during the nephrographic phase. Aliasing artifacts were more pronounced on DL-CAIPIRINHA-VIBE, particularly when the field-of-view (FOV) was not large enough. This effect can be mitigated when planning the sequence and adjusting the FOV accordingly. Pronounced aliasing artifacts could potentially hamper overall image quality. But since these artifacts were mild in our study, we did not find that they significantly impacted overall image quality or diagnostic confidence in the assessment of renal lesions. Also, the on a quantitative level, RRC and lesion size was similar between standard and DL-CAIPIRINHA VIBE. In the subset of solid renal lesions, RRC was higher for DL-CAIPIRINHA-VIBE. A possible explanation for this may be the scan order of our protocol, which acquired the standard CAIPIRINHA-VIBE axial prior to the DL-CAIPIRINHA-VIBE, resulting in a slightly later phase for the study sequence, potentially increasing the contrast between the solid tumors and the renal parenchyma.

Recent studies have evaluated similar DL-based 3D T1w GRE sequences to evaluate various abdominal and pelvic diseases with optimistic results [15,16,30]. Similarly, our study was able to show that DL-CAIPIRINHA-VIBE performs well for kidney imaging, further illustrating the versatility of the DL-algorithm. This is especially remarkable, as the algorithm was trained on data from healthy volunteers, which could have potentially limited its' application for kidney imaging.

Our study had several limitations. First, as a single institution prospective investigation, there might be inherent selection bias. Second, we utilized a single vendor 3 T MRI (MAGNETOM Vida, Siemens Healthineers, Germany). Hence, our findings might not be universally applicable across different vendors and field strengths. Third, the relatively small sample size and number of renal lesions may constrain the statistical power of our findings. Fourth, we measured only RRC and subjectively assessed perceived noise. We refrained from conducting other quantitative measurements of noise, as these might be unreliable when performed with conventional ROI measurements of noise level, especially when parallel acquisition techniques or non-linear reconstruction methods like DL-based algorithms are involved [31].

5. Conclusions

In conclusion, DL-CAIPIRINHA-VIBE in the nephrographic phase greatly enhances overall image quality and reduces movement and breathing artifacts. Although DL-CAIPIRINHA-VIBE showed more obvious aliasing artifacts and an apparent synthetic appearance, these factors were not significantly detrimental to the overall image quality and superior diagnostic confidence in the assessment of renal lesions in our study, when compared to a standard CAIPIRINHA-VIBE.

Ethics approval and consent to participate

The Charité Ethikkommission (Charité Universitätsmedizin Berlin) approved the prospective study. Informed conset was obtained from all participants.

Authors' contributions

Q.T. and J.M. read the data

Q.T. and J.M. wrote the first draft of the manuscript, prepared figures and tables

L.N. and M.L. enrolled patients and aided data acquisition

S.H. and R.P. referred patients and provided clinical data

T.P. and Q.T. performed statistical analyses

D. N. and M.W. conceptualized the study methodology

T.W. interpreted the data, edited and finalized the manuscript, prepared tables and figures and was a major contributor to the final manuscript

Funding

There's a research agreement and funding in place between Siemens Healthineers and the Institution.

T.P. is also funded in part by the Berlin Institute of Health (BIH). T.P. also declares relationships with the following companies: research agreements (no personal payments) with AGO, Aprea AB, ARCAGY-GINECO, Astellas Pharma Global Inc. (APGD), Astra Zeneca, Clovis Oncology, Inc., Holaira, Incyte Corporation, Karyopharm, Lion Biotechnologies, Inc., MedImmune, Merck Sharp & Dohme Corp, Millennium Pharmaceuticals, Inc., Morphotec Inc., NovoCure Ltd., PharmaMar S.A. and PharmaMar USA, Inc., Roche, Siemens Healthineers, and TESARO Inc., and fees for a book translation (Elsevier B.V.).

T.P. is also funded in part by the Berlin Institute of Health (BIH). T.P. also receives funding from Berlin Institute of Health (Advanced Clinician Scientist Grant, Platform Grant), Ministry of Education and Research (BMBF, 01KX2021 (RACOON), 01KX2121 („NUM 2.0", RACOON), 68GX21001A, 01ZZ2315D), German Research Foundation (DFG, SFB 1340/2), European Union (H2020, CHAIMELEON: 952172, DIGITAL, EUCAIM:101100633).

B.H. is the editor in chief of European Radiology (ESR). B.H. also reports grant money from companies or nonprofit organizations to the Department of Radiology (outside of submitted work) from Abbott, Actelion Pharmaceuticals, Bayer Schering Pharma, Bayer Vital, BRACCO Group, Bristol-Myers Squibb, Charité Research Organization GmbH, Krebshilfe, Stiftung für Herzforschung, Essex Pharma, EU Programmes, Fibrex Medical Inc., Focused Ultrasound Surgery Foundation, Fraunhofer Gesellschaft, Guerbet, INC Research, InSightec Ltd., IPSEN Pharma, Kendle/MorphoSys AG, Lilly GmbH, Lundbeck GmbH, MeVis Medical Solutions AG, Nexus Oncology, Novartis, Parexel CRO Service, Perceptive, Pfizer GmbH, Philipps, Sanofi-Aventis S.A, Siemens, Spectranetics GmbH, Terumo Medical Corporation, TNS Healthcare GmbH, Toshiba, UCB Pharma, Wyeth Pharma and Zukunftsfond Berlin (TSB).

B.H. also reports grant money from companies or nonprofit organizations to the Department of Radiology (outside of submitted work) from Abbott, Actelion Pharmaceuticals, Bayer Schering Pharma, Bayer Vital, BRACCO Group, Bristol-Myers Squibb, Charité Research Organization GmbH, Krebshilfe, Stiftung für Herzforschung, Essex Pharma, EU Programmes, Fibrex Medical Inc., Focused Ultrasound Surgery Foundation, Fraunhofer Gesellschaft, Guerbet, INC Research, InSightec Ltd., IPSEN Pharma, Kendle/MorphoSys AG, Lilly GmbH, Lundbeck GmbH, MeVis Medical Solutions AG, Nexus Oncology, Novartis, Parexel CRO

Service, Perceptive, Pfizer GmbH, Philipps, Sanofi-Aventis S.A, Siemens, Spectranetics GmbH, Terumo Medical Corporation, TNS Healthcare GmbH, Toshiba, UCB Pharma, Wyeth Pharma and Zukunftsfond Berlin (TSB).

T.W.C reports payments from Bayer outside the scope of the current work.

CRediT authorship contribution statement

Thula Cannon Walter-Rittel: Writing – review & editing, Validation, Supervision, Methodology. **Qinxuan Tan:** Writing – original draft, Formal analysis, Data curation. **Jingyu Miao:** Writing – original draft, Visualization, Investigation, Data curation. **Leila Nitschke:** Investigation, Data curation. **Dominik Geisel:** Conceptualization, Resources. **Moritz Wagner:** Supervision, Resources, Project administration, Investigation, Funding acquisition, Conceptualization. **Robert Peters:** Data curation. **Bernd Hamm:** Resources. **Tobias Penzkofer:** Validation, Investigation. **Marcel Dominik Nickel:** Software, Resources, Methodology. **Markus Herbert Lerchbaumer:** Methodology, Data curation. **Sebastian Hofbauer:** Data curation.

Declaration of Competing Interest

There's a research agreement in place between Siemens Healthineers and the Institution. D.N. is an employee at Siemens Healthineers.

Acknowledgements

Not applicable.

Consent for publication

"Not applicable"

Clinical relevance statement

Contrast enhanced DL-CAIPIRINHA VIBE in the nephrogenic phase is well suited for the evaluation of renal lesions and improves overall image quality compared to standard CAIPIRINHA VIBE.

Data availability

The data is available from the authors upon reasonable request.

References

[1] R.D. Ward, et al., 2017 AUA renal mass and localized renal cancer guidelines: imaging implications, Radiographics 38 (7) (2018) 2021–2033.
[2] A.C. Tsili, et al., The role of imaging in the management of renal masses, Eur. J. Radio. 141 (2021) 109777.
[3] J.J. Nikken, G.P. Krestin, MRI of the kidney-state of the art, Eur. Radio. 17 (11) (2007) 2780–2793.
[4] J.G. Fried, M.A. Morgan, Renal imaging: core curriculum 2019, Am. J. Kidney Dis. 73 (4) (2019) 552–565.
[5] V.B. Ho, et al., Renal masses: quantitative assessment of enhancement with dynamic MR imaging, Radiology 224 (3) (2002) 695–700.
[6] S. Huber, et al., Comparison of image quality of subtracted and nonsubtracted breath hold VIBE and free breathing GRASP in the evaluation of renal masses, Clin. Imaging 74 (2021) 15–18.
[7] M. Seo, et al., Image quality of high-resolution 3-dimensional neck MRI using CAIPIRINHA-VIBE and GRASP-VIBE: an intraindividual comparative study, Invest Radio. 57 (11) (2022) 711–719.
[8] H. Chandarana, et al., Free-breathing radial 3D fat-suppressed T1-weighted gradient echo sequence: a viable alternative for contrast-enhanced liver imaging in patients unable to suspend respiration, Invest Radio. 46 (10) (2011) 648–653.
[9] N. Jin, H. Saybasili, X. Bi, Spatial, Temporal Resolution and Signal-to-Noise Ratio, in: M.A. Syed, S.V. Raman, O.P. Simonetti (Eds.), in *Basic Principles of Cardiovascular MRI: Physics and Imaging Technique*, Springer International Publishing, Cham, 2015, pp. 41–62.
[10] S. Gassenmaier, et al., Deep learning applications in magnetic resonance imaging: has the future become present? Diagn. (Basel) 11 (12) (2021).
[11] S. Gassenmaier, et al., Image quality improvement of dynamic contrast-enhanced gradient echo magnetic resonance imaging by iterative denoising and edge enhancement, Invest Radio. 56 (7) (2021) 465–470.
[12] J. Herrmann, et al., Diagnostic confidence and feasibility of a deep learning accelerated HASTE sequence of the abdomen in a single breath-hold, Invest Radio. 56 (5) (2021) 313–319.
[13] D.H. Kim, et al., Deep learning-accelerated liver diffusion-weighted imaging: intraindividual comparison and additional phantom study of free-breathing and respiratory-triggering acquisitions, Invest Radio. 58 (11) (2023) 782–790.
[14] H. Almansour, et al., Deep learning-based superresolution reconstruction for upper abdominal magnetic resonance imaging: an analysis of image quality, diagnostic confidence, and lesion conspicuity, Invest Radio. 56 (8) (2021) 509–516.
[15] M. Chaika, et al., Deep learning-based super-resolution gradient echo imaging of the pancreas: Improvement of image quality and reduction of acquisition time, Diagn. Inter. Imaging 104 (2) (2023) 53–59.
[16] J.H. Son, et al., LAVA HyperSense and deep-learning reconstruction for near-isotropic (3D) enhanced magnetic resonance enterography in patients with Crohn's disease: utility in noise reduction and image quality improvement, Diagn. Inter. Radio. 29 (3) (2023) 437–449.
[17] H. Wei, et al., Enhancing gadoxetic acid-enhanced liver MRI: a synergistic approach with deep learning CAIPIRINHA-VIBE and optimized fat suppression techniques, Eur. Radio. 34 (10) (2024 Oct) 6712–6725.
[18] K. Hammernik, et al., Learning a variational network for reconstruction of accelerated MRI data, Magn. Reson Med 79 (6) (2018) 3055–3071.
[19] U.L. Fahlenkamp, et al., Improved visualisation of hepatic metastases in gadoxetate disodium-enhanced MRI: Potential of contrast-optimised (phase-sensitive) inversion recovery imaging, PLoS One 14 (3) (2019) e0213408.
[20] M. Benchoufi, et al., Interobserver agreement issues in radiology, Diagn. Inter. Imaging 101 (10) (2020) 639–641.
[21] U. Kramer, et al., Isotropic high-spatial-resolution contrast-enhanced 3.0-T MR angiography in patients suspected of having renal artery stenosis, Radiology 247 (1) (2008) 228–240.
[22] I. Pedrosa, et al., MR imaging of renal masses: correlation with findings at surgery and pathologic analysis, Radiographics 28 (4) (2008) 985–1003.
[23] J. Hamilton, D. Franson, N. Seiberlich, Recent advances in parallel imaging for MRI, Prog. Nucl. Magn. Reson Spectrosc. 101 (2017) 71–95.
[24] N.M. Rofsky, et al., Abdominal MR imaging with a volumetric interpolated breath-hold examination, Radiology 212 (3) (1999) 876–884.
[25] H. Yang, K. Rose, Optimizing motion compensated prediction for error resilient video coding, IEEE Trans. Image Process 19 (1) (2010) 108–118.
[26] M.H. Yu, et al., Clinical application of controlled aliasing in parallel imaging results in a higher acceleration (CAIPIRINHA)-volumetric interpolated breathhold (VIBE) sequence for gadoxetic acid-enhanced liver MR imaging, J. Magn. Reson Imaging 38 (5) (2013) 1020–1026.
[27] F.A. Breuer, et al., Controlled aliasing in parallel imaging results in higher acceleration (CAIPIRINHA) for multi-slice imaging, Magn. Reson Med 53 (3) (2005) 684–691.
[28] M.H. Albrecht, et al., Intra-individual comparison of CAIPIRINHA VIBE technique with conventional VIBE sequences in contrast-enhanced MRI of focal liver lesions, Eur. J. Radio. 86 (2017) 20–25.
[29] S. Afat, et al., Analysis of a deep learning-based superresolution algorithm tailored to partial fourier gradient echo sequences of the abdomen at 1.5 t: reduction of breath-hold time and improvement of image quality, Invest Radio. 57 (3) (2022) 157–162.
[30] D. Wessling, et al., Application of a deep learning algorithm for combined super-resolution and partial fourier reconstruction including time reduction in T1-weighted precontrast and postcontrast gradient echo imaging of abdominopelvic MR imaging, Diagn. (Basel) 12 (10) (2022).
[31] O. Dietrich, et al., Measurement of signal-to-noise ratios in MR images: influence of multichannel coils, parallel imaging, and reconstruction filters, J. Magn. Reson Imaging 26 (2) (2007) 375–385.